Received: 22 February 2024 | Revised: 24 April 2024 | Accepted: 13 May 2024

DOI: 10.1111/cge.14563

ORIGINAL ARTICLE

CLINICAL GENETICS WILEY

Expanding the spectrum of phenotypes for *MPDZ*: Report of four unrelated families and review of the literature

Aboulfazl Rad[1] | Oliver Bartsch[2] | Somayeh Bakhtiari[3,4] | Changlian Zhu[5,6] | Yiran Xu[6] | Fabíola P. Monteiro[7] | Fernando Kok[7,8] | Anneke T. Vulto-van Silfhout[9,10] | Michael C. Kruer[3,4] | Michael R. Bowl[11] | Barbara Vona[1,12,13]

[1]Department of Otolaryngology – Head and Neck Surgery, Tübingen Hearing Research Centre, Eberhard Karls University Tübingen, Tübingen, Germany

[2]Medical Care Centre Section Human Genetics and Institute of Human Genetics, University Medical Centre of the Johannes Gutenberg University Mainz, Mainz, Germany

[3]Barrow Neurological Institute, Phoenix Children's Hospital, Phoenix, Arizona, USA

[4]Department of Child Health, Cellular and Molecular Medicine, Genetics, and Neurology, University of Arizona College of Medicine-Phoenix, Phoenix, Arizona, USA

[5]Center for Brain Repair and Rehabilitation, Institute of Neuroscience and Physiology, University of Gothenburg, Göteborg, Sweden

[6]Henan Key Laboratory of Child Brain Injury and Henan Pediatric Clinical Research Center, Institute of Neuroscience and Third Affiliated Hospital of Zhengzhou University, Zhengzhou, China

[7]Medical Department, Mendelics Genomic Analysis, Sao Paulo, Brazil

[8]Neurogenetics, Neurology Department, Hospital das Clínicas da Universidade de São Paulo, São Paulo, Brazil

[9]Department of Human Genetics, Radboud University Medical Centre, Nijmegen, the Netherlands

[10]Department of Clinical Genetics, Maastricht University Medical Center, Maastricht, the Netherlands

[11]UCL Ear Institute, University College London, London, UK

[12]Institute of Human Genetics, University Medical Center Göttingen, Göttingen, Germany

[13]Institute for Auditory Neuroscience and InnerEarLab, University Medical Center Göttingen, Göttingen, Germany

Correspondence
Barbara Vona, Institute of Human Genetics, Institute for Auditory Neuroscience and InnerEarLab, University Medical Center Göttingen, Göttingen, Germany.
Email: barbara.vona@med.uni-goettingen.de

Funding information
Medizinischen Fakultät, Eberhard Karls Universität Tübingen, Grant/Award Number: 2545-1-0; Ministerium für Wissenschaft, Forschung und Kunst Baden-Württemberg; Deutsche Forschungsgemeinschaft VO 2138/7-1, Grant/Award Number: 469177153; National Natural Science Foundation of China, Grant/Award Number: U21A20347

Abstract

MPDZ, a gene with diverse functions mediating cell–cell junction interactions, receptor signaling, and binding multivalent scaffold proteins, is associated with a spectrum of clinically heterogeneous phenotypes with biallelic perturbation. Despite its clinical relevance, the mechanistic underpinnings of these variants remain elusive, underscoring the need for extensive case series and functional investigations. In this study, we conducted a systematic review of cases in the literature through two electronic databases following the PRISMA guidelines. We selected nine studies, including 18 patients, with homozygous or compound heterozygous variants in *MPDZ* and added five patients from four unrelated families with novel *MPDZ* variants. To evaluate the role of *Mpdz* on hearing, we analyzed available auditory electrophysiology data from a knockout murine model (*Mpdz*$^{em1(IMPC)J/em1(IMPC)J}$) generated by the International Mouse Phenotyping Consortium. Using exome and genome sequencing, we identified three families with compound heterozygous variants, and one family with a

homozygous frameshift variant. *MPDZ*-related disease is clinically heterogenous with hydrocephaly, vision impairment, hearing impairment and cardiovascular disease occurring most frequently. Additionally, we describe two unrelated patients with spasticity, expanding the phenotypic spectrum. Our murine analysis of the *Mpdz*$^{em1(IMPC)J/em1(IMPC)J}$ allele showed severe hearing impairment. Overall, we expand understanding of *MPDZ*-related phenotypes and highlight hearing impairment and spasticity among the heterogeneous phenotypes.

KEYWORDS
hearing loss, hydrocephaly, MPDZ, phenotypic heterogeneity, spasticity

1 | INTRODUCTION

MPDZ, also known as *MUPP1* (OMIM: 603785), encodes the multiple PDZ domain crumbs cell polarity complex component. This protein stands as the largest among PDZ (PSD95/DLG1/ZO1) domain-containing proteins, with 13 PDZ domains. Its initial discovery originated from interaction with the HTR2C serotonin receptor from a yeast 2-hybrid screen using human fetal brain cDNA.[1,2] PDZ domain proteins represent a diverse and abundant family of interaction domain scaffolding proteins, and they fulfill crucial roles across various cellular contexts, orchestrating intricate networks of interactions. This expansive network involves interactions with more than 15 proteins, encompassing members of the tight junctions protein family, G protein-coupled receptors (GPCRs), SynGAP, and CaMKII at synapses,[3,4] as well as delta like protein 1 and 4 (DLL1/4) and NECTIN2 at epithelial apical junctions.[5]

The *MPDZ* gene-disease relationship with biallelic variants currently extends to congenital hydrocephalus type 2 with or without brain or eye abnormalities (OMIM: 615219); however, the literature presents a continuously evolving and complex phenotypic landscape. Functional studies have contributed to our understanding of the phenotypic manifestations linked to *MPDZ*. For instance, Feldner et al. used a mouse model (*Mpdz*$^{-/-}$) revealing that *Mpdz* depletion impairs multiple ependymal functions, potentially leading to perinatal-onset hydrocephalus.[6] Yang et al. identified a crucial role of *Mpdz* in the choroid plexus, where choroid plexus hyperpermeability, attributed to *Mpdz* deficiency, precipitated hydrocephalus in a *Mpdz*$^{-/-}$ murine model.[7] Jarysta and Tarchini[8] uncovered a novel functional importance of MPDZ in cochlear hair cell development. Interestingly, MPDZ expression was not localized to the apical cell junctions in the epithelium but rather at the hair cell apical membrane. *Mpdz* mutants exhibited misaligned stereocilia placement and dysmorphic hair bundles.[8]

Due to the manifold and expanding clinical and genetic data described, we sought to address this complexity by presenting a case-series comprising four unrelated families with biallelic *MPDZ* variants. Additionally, we reviewed the existing literature to compile a detailed report on the wide array of phenotypes associated with *MPDZ* variants. We also analyzed auditory phenotyping data from a murine model. Our results reaffirm the role of *MPDZ* in hearing impairment and spasticity while contributing new information about the clinical landscape resulting from biallelic *MPDZ* variants.

2 | METHODS

2.1 | Patient recruitment

This study was approved by the University of Tübingen Ethics Commission, No. 197/2019BO1 and the University Medical Center Göttingen, local institutional ethics board, No. 3/2/16. Four unrelated families presenting a variety of clinical indications were aggregated from four different centers by direct communication or via GeneMatcher.[9] Blood samples were collected after obtaining informed consent from patients or their parents. Informed consent from the parents or legal guardians of the patients/participants was obtained for the publication of their data.

2.2 | Literature search strategy and selection criteria

Electronic bibliographic databases including PubMed (https://pubmed.ncbi.nlm.nih.gov/ accessed on 11 February 2024) and Web of Science (https://www.webofscience.com/ accessed on February 11, 2024) were used for the literature search. The search strategy used the keyword "MPDZ" for each database. We used EndNote 21 (https://endnote.com/ accessed on January 9, 2024) to collect all the results in a single library.

Our inclusion criteria encompassed publications that reported patients with suspected deleterious homozygous, and compound heterozygous variants in *MPDZ*. The exclusion criteria were: (i) duplicate publications; (ii) studies unrelated to the scope of this paper; (iii) reports in the form of abstracts, reviews, theses, and conference papers; and (iv) studies describing patients with heterozygous or homozygous variants in *MPDZ* classified as likely benign based on ACMG/ClinGen criteria.

The full text of all the potentially eligible articles and their supplementary information were obtained by two authors (AR and BV) working independently.

2.3 | Sequencing, bioinformatics analysis, and variant classification

Following extraction of DNAs from whole blood by standard protocol, proband DNA samples were subjected to exome capture using either the Agilent SureSelect Human All Exon V6 Kit (Families 1 and 3), or the Nextera Exome Capture (Family 2), or genome enrichment with the Illumina DNA PCR free Prep Kit (Family 4). Exome sequencing (ES) was performed on an Illumina HiSeq 2500 sequencer for an average 50× sequencing depth, resulting in sequences of greater than 100 bases from each end of the fragments. The proband of Family 1 was sequenced at the Institute of Human Genetics, University Medical Centre of the Johannes Gutenberg University Mainz, Family 2 at Mendelics Genomic Analysis, and Family 3 at Zhengzhou University. For Family 4, the genome sequencing was performed on the Illumina NovaSeq 6000 at the Radboud University Medical Centre, Nijmegen, the Netherlands. Read alignment and variant calling were performed using DRAGEN Bio-IT Platform (Illumina). Exome data were processed for analysis using a GATK-based pipeline[10] that used Burrows-Wheeler alignment[11] to the GRCh37/UCSC hg19 human genome assembly. Single nucleotide variant and InDel detection utilized VarScan version 2.2.5, MuTec and GATK Somatic Indel Detector. A previously described protocol aided interpretation of potentially pathogenic variants.[12] gnomAD v4.0.0[13] was used for population-specific filtering. The prediction of two in silico tools including REVEL[14] and CADD[15] were used to assess the pathogenicity of variants. All variants were classified based on ACMG and ClinGen Sequence Interpretation (SVI) Working Group guidelines.

Segregation analysis using Sanger sequencing was performed in available family members of Families 1, 2, and 3 to confirm variant segregation after polymerase chain reaction (PCR) amplification. Primers are available upon request.

2.4 | Splice variant prediction and in vitro splicing assay

Prediction of aberrant splicing used Alamut Genova v.1.4, employing SpliceSiteFinder-like, MaxEntScan, NNSPLICE and GeneSplicer. A mini-gene splice assay was done as previously described[16,17] to assay splice effects of the c.5231+1G>A variant. Briefly, PCR amplicons were generated from the genomic DNAs of an affected (Family 1, II-2) and wild-type individual (mother, I-2) using a forward primer with a *Xho*I restriction site (MPDZ Ex3 *Xho*I F: 5′-aattctcgag-TAATTTTTGGCCCACTACCC-3′) and a reverse primer with a *Bam*HI restriction site (MPDZ Ex3 *Bam*HI R: 5′-attggatccCCTTCGTTGCA-TAAGGATGAC-3′). The 1176 bp amplicon included the entire genomic region spanning exons 37 and 38, as well as additional flanking 320 bp (5′) and 306 bp (3′) sequence that was ligated into a multiple cloning site between native exons A and B in the linearized pSPL3 exon-trapping vector. The vector was transformed into DH5α competent cells and plated overnight. All mutant mini-genes were Sanger sequence confirmed.

Homozygous and wild-type mini-genes were transfected in triplicate into HEK 293T cells cultured in FBS-free medium in 12 well culture plates with a density of 1×10^5 cells per mL. The mini-genes in the pSPL3 vector were transiently transfected using 3 µL of FuGENE 6 Transfection Reagent (Roche) with 1 µg of vector. An empty vector and HEK 293T cells were included as controls. The transfected cells were harvested 24 h post-transfection. Total RNA was prepared using the miRNAeasy Mini Kit (Qiagen). Approximately 500 ng of RNA was reverse transcribed using a High-Capacity RNA-to-cDNA Kit (Applied Biosystems) following manufacturer's protocols. The cDNA was used for PCR amplification using a vector specific SD6 forward (5′-TCTGAGTCACCTGGACAACC-3′) and a terminal *MPDZ* exon 3 reverse cDNA primer (5′-CAAGATATCCTCAGCTGTGACC-3′). The resulting amplified fragments were visualized on a 1.5% agarose gel. cDNA amplicons were Sanger sequenced. Individual cDNA amplicons from the c.5231+1G>A variant were TA-cloned following standard protocols (dual promoter with pCRII, Invitrogen).

3 | RESULTS

3.1 | Review of the literature

The systematic review of literature considered 162 abstracts. Following adherence to inclusion and exclusion criteria, nine studies remained that reported patients with biallelic *MPDZ* variants who were analyzed in detail for clinical information. The PRISMA flowchart summarizes the process of identification and selection of nine publications describing 18 patients (Figure 1). Additionally, we incorporated data from five patients from four unrelated families, resulting in 23 patients (10 [43.5%] male, 6 [26.1%] female, 5 [21.7%] fetuses, and 2 [8.7%] no information available).

The analysis revealed the presence of 25 distinct homozygous or heterozygous variants distributed across 15 exons and 3 introns of *MPDZ*. Sixteen out of 25 were located within the 13 PDZ domains of MPDZ. Notably, in individuals with severe phenotypes, at least one variant was located within the PDZ domain (Table S1).

3.2 | Clinical spectrum of phenotypes associated with biallelic *MPDZ* variants

Patients with *MPDZ* variants exhibited a wide range of clinical phenotypes (Table 1). The literature reports 23 patients with ages ranging from fetal stage to 43 years old. Among these patients, 12 (52.2%) presented hydrocephalus, ranging from lethal to mild, with three patients characterized as mild. Al-Dosari et al.[27] initially described two patients with severe hydrocephalus, labeling the condition as non-syndromic hydrocephalus. However, a broader phenotypic constellation was subsequently identified in patients with *MPDZ*-related disorders. Nine patients (39.1%) exhibited various forms of vision impairment. Recently, two separate reports described vision impairment as including macular coloboma as well as bilateral macular

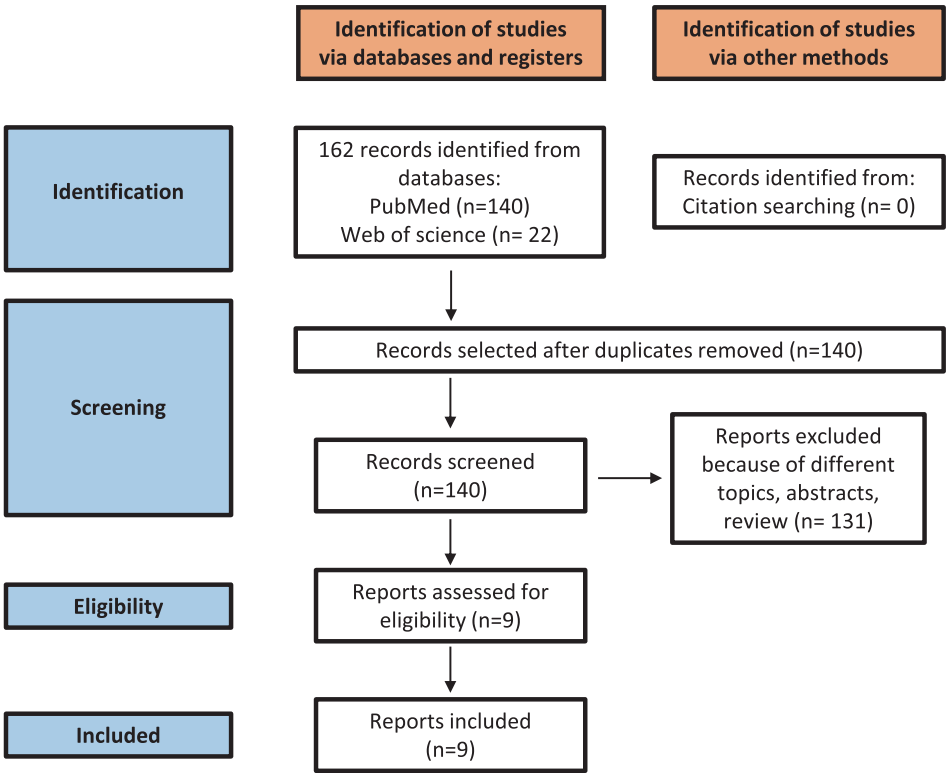

FIGURE 1 PRISMA flowchart of the literature review. [Colour figure can be viewed at wileyonlinelibrary.com]

colobomas with symmetric patches of chorioretinal atrophy in the temporal periphery, respectively. Six patients (26.1%) were described as having congenital hearing impairment, varying from mild to profound. Interestingly, two Pakistani siblings had hearing loss due to a biallelic variant in *MPDZ*. Another patient with the same variant (c.2324C>T, p.Pro775Leu) and non-syndromic hearing loss was also reported in ClinVar (variation ID: 995976). Cardiovascular abnormalities were observed in four (17.4%) patients with various phenotypes, including congenital heart defects, aberrant subclavian artery, and portal vein thrombosis. Seven (30.4%) patients had macrocephaly, and three (13.0%) had frontal bossing. Skeletal anomalies, such as persistent fetal pads and striking creases over the knee, as well as joint hypermobility, were seen in two patients (8.7%) each. Two patients each (8.7%) exhibited hypotonia and spasticity. Three patients (13.0%) had intellectual disability, and three patients (13.0%) experienced seizures. In a study by Shaheen et al., one patient was identified with intrahepatic cholestasis and multicystic dysplastic kidney; however, this patient had a variant in *TJP2* (classified likely pathogenic based on ACMG guidelines) explaining these phenotypes.[25]

3.3 | Clinical assessment

We studied four unrelated families originating from various global regions (Europe, South America, and Asia), each displaying a variety of phenotypes including hydrocephaly, seizure, spastic paraparesis, hearing loss, cardiac abnormalities and vision impairment.

3.4 | Family 1

The female proband (II-2) in Family 1, patient 1 in Table 1, is one of two living affected children out of three children, delivered at term to non-consanguineous parents (Figure 2A). Hydrocephalus was first noted prenatally in the 27th week of gestation. She was born at 34 gestational weeks with marked primary hydrocephalus and occipital frontal circumference (OFC) 42 cm (>99th percentile + 6z). She exhibited delayed speech development, virtually not speaking at all until age 5 years and was initially suspected to have congenital hearing loss that was clinically diagnosed as mild to moderate sensorineural hearing loss. At age 5 years, she received hearing aids, which significantly improved her speech. At age 6 years and 3 months, height was 117 cm (31st percentile), weight was 16.5 kg (2nd percentile −2.1z) and OFC was 53 cm (92nd percentile +1.4z). She had a developmental delay of approximately 30% of her age, suggesting learning disability or mild intellectual disability. The youngest daughter (II-3) in this family was delivered at term and similarly had prenatal hydrocephalus detected in week 22+2 of gestation. She failed universal newborn hearing screening. An older female sibling had died at age 8 months but evidence is too sparse to include or exclude as a same disease in this family.

3.5 | Family 2

The proband in Family 2 is a 43-year-old female, the youngest of four siblings born to non-consanguineous parents (Figure 2A). Family

TABLE 1 Description of phenotype and genotype of 24 selected patients.

	Number/ sex/ ethnicity	Variant	Age of last examination	Hydrocephalus	Vision impairment	Hearing loss	Cardiovascular	Macrocephaly/ frontal bossing/ skeletal anomalies	Seizure/ Intellectual disability/MRI	Spasticity/ hypotonia	Detailed clinical information
Current study (Family 1, II.2)	1/F/ German	c.3508C>T, p.Arg1170* (mat), c.5231+1G>A p.? (pat)	6 years	Yes	No	Yes	No	Yes/Yes/No	No/No/NA	No/No	Primary hydrocephaly, congenital mild to moderate sensorineural hearing loss
Current study (Family 1, II.3)	2/F/ German	c.3508C>T, p.Arg1170*(mat), c.5231+1G>A p.? (pat)	1 year	Yes	No	Yes	No	Yes/No/No	No/No/NA	No/No	Primary hydrocephaly, congenital mild to moderate sensorineural hearing loss
Current study (Family 2, II.4)	3/F/ Brazilian	c.1026dup p.Ala343Serfs*22 (pat), c.4993G>A p.Ala1665Thr (mat)	43 years	No, but mild ex-vacum ventricle enlargement	Yes	No	No	No/No/No	No/No/ Remarkable	Yes/No	Bilaterally increased P100 wave latency with normal amplitude on VEP, ABR disclosing widened I–V interpeak interval on the left ear. No abnormalities on the right ear; Sinus arrhythmia; MRI—bilateral tenuous T2 and Flair white matter hyperintensities in the cerebral hemispheres and anterior portion of the corpus callosum, and mild "ex-vacum" lateral ventricle enlargement
Current study (Family 3, II.1)	4/M/Han Chinese	c.5362G>C p.Val1788Leu (mat), c.5701G>C p.Val1901Leu (pat)	3 years	No	No	No	No	No/No/No	No/No/NA	Yes/No	NA
Current study (Family 4, II.1)	5/M/NA	c.4282_4288del p.Ile1428Serfs*7	4 years	Yes	Yes	No	No	Yes/Yes/No	Yes/Yes/ Remarkable	No/No	Septo-optic dysplasia, antenatal hydrocephalus, bilateral macular colobomas
Iyengar et al. (2022)[18]	6/M/NA	c.3100C>T p.Arg1034* (mat), c.747+2T>G, p.? (pat)	4 years	No	Yes	No	No	No/No/No	No/No/NA	No/No	Bilateral macular colobomas with symmetric patches of chorioretinal atrophy in the temporal periphery; another sister died at 1 month of age secondary to an unknown cardiovascular issue, but records are unavailable
Iyengar et al. (2022)[18]	7/M/NA	c.3100C>T p.Arg1034* (mat), c.747+2T>G, p.? (pat)	9 years	No	Yes	No	No	No/No/No	No/No/NA	No/No	Subtle thinning of the temporal fovea in both eyes

(Continues)

TABLE 1 (Continued)

	Number/ sex/ ethnicity	Variant	Age of last examination	Hydrocephalus	Vision impairment	Hearing loss	Cardiovascular	Macrocephaly/ frontal bossing/ skeletal anomalies	Seizure/ Intellectual disability/MRI	Spasticity/ hypotonia	Detailed clinical information
Zhang et al. (2022)[19]	8/M/ Chinese	c.4301delA p.Asp1434fs*3 (mat), c.5255C>G p.Ser1752* (pat)	26 years	No	Yes	No	No	No/No/No	No/No/NA	No/No	Macular coloboma; One deceased sibling with unknown reason of death
Bharadwaj et al. (2022)[20]	9/ F/Pakistani	c.2324C>T p.Pro775Leu	NA	No	No	Yes	No	No/No/No	No/No/NA	No/No	Congenital profound sensorineural hearing loss
Bharadwaj et al. (2022)[20]	10/ M/Pakistani	c.2324C>T p.Pro775Leu	NA	No	No	Yes	No	No/No/No	No/No/NA	No/No	Congenital profound sensorineural hearing loss
Bertolli et al. (2021)[21]	11/NA/NA	c.3253A>T p.Lys1085*	NA	NA	NA	NA	Yes	NA/NA/NA	NA/NA/NA	NA/NA	Ventricular septal defect, atrial septal defect, secundum atrial septal defect, ventriculomegaly, abnormality of the septum pellucidum, antenatal onset
Moazzeni et al (2020)[22]	12/ F/Iranian	c.409G>T p.Val137Phe	NA	No	Yes	Yes	No	No/No/No	No/No/NA	No/No	Congenital hereditary endothelial dystrophy, congenital mild sensorineural hearing loss
Al-Jezawi et al. (2018)[23]	13/M/ Emirati	c.394G>A p.Gly132Ser (mat), c.1744C>G p.Leu582Val (pat)	9 months	Yes	No	No	No	Yes/Yes/No	No/No/ Remarkable	No/No	The brother of the mother has a daughter with hydrocephalus and VP shunt. MRI: widened CSF spaces in the frontoparietal region bilaterally and mild dilation of lateral and third ventricles
Harripaul et al. (2018)[24]	14/M/NA	c.5898_5901del, p.Phe1967Leufs*3	NA	No	No	No	No	No/No/No	No/Yes/NA	No/No	NA
Shaheen et al. (2017)[25]	15/M/ Saudi	c.628C>T p.Gln210*	NA	Yes	No	No	No	Yes/No/No	No/Yes/NA	No/No	One affected brother with severe hydrocephalus died 1 day after delivery, no more information is available for this sibling
Shaheen et al. (2017)[25]	16/F/ Palestinian	c.4469del p.Gln1490Argfs*19	2.5 years	Yes	No	No	Yes	No/Yes/Yes	No/No/ Remarkable	No/No	Aberrant subclavian artery, moderate ASD; MRI: dilatation of the lateral ventricles and the third ventricle; asymmetric face and bulbous nose, delayed motor development, congenital diaphragmatic hernia

TABLE 1 (Continued)

	Number/ sex/ ethnicity	Variant	Age of last examination	Hydrocephalus	Vision impairment	Hearing loss	Cardiovascular	Macrocephaly/ frontal bossing/ skeletal anomalies	Seizure/ Intellectual disability/MRI	Spasticity/ hypotonia	Detailed clinical information
Shaheen et al. (2017)[25]	17/M/Scot-Irish-Dutch	c.2230C>T p.Arg744* (NA), c.3211C>T p.Arg1071* (NA)	8 years	Yes	Yes	Yes	Yes	No/No/Yes	No/No/ Remarkable	No/No	Foveal dysplasia, thin inner retina, bilateral lacrimal ducts stenosis; sensorineural hearing loss; aberrant subclavian artery, portal vein thrombosis; MRI: small olfactory bulbs, minimal dilatation of the lateral brain ventricles, multiple bilateral foci of subependymal nodular gray matter heterotopia and enlarged massa intermedia; lung hypoplasia; small teeth, two posterior hair whorls, lung hypoplasia, malrotation of gut, downslanting palpebral fissures, posteriorly rotated ears
Shaheen et al. (2017)[25]	18/ M/Kuwait	c.5278G>A p.Ala1760Thr	15 months	Yes	Yes	No	No	Yes/No/No	No/No/ Remarkable	No/Yes	Iris coloboma, Prominent optic nerve; MRI: enlarged third and lateral ventricles and extra-axial spaces, and increased signal intensity within the central tegmental tracts and frontal horns; progressive familial Intrahepatic cholestasis (this was because of *TJP2*), multicystic dysplastic kidney
Saugier-Veber et al. (2017)[26]	19/Fetus/ Senegalese	c.1291_1294del p.Val431Metfs*14	Terminate at 30 WG.	NA	NA	NA	NA	Yes/No/No	NA/NA/ Remarkable	NA/NA	MRI: at 28 weeks gestation confirmed massive hydrocephalus
Saugier-Veber et al (2017)[26]	20/Fetus/ NA	c.533+1G>T p.?	Terminated at 29 and 25 WG	Yes	NA	NA	NA	NA/NA/NA	NA/NA/NA	NA/NA	Affected sibling was delivered 35 weeks gestation with 2920 g weight, 41.5 cm (95 percentile), soon after birth underwent ventricular shunting, but died a few weeks later from meningoencephalitis
Saugier-Veber et al. (2017)[26]	21/Fetus/ NA	c.2248C>T p.Arg750*	Terminated at 29 and 25 WG	Yes	NA	NA	NA	NA/NA/NA	NA/NA/NA	NA/NA	All three terminations were done because of severe isolated recurrent hydrocephalus

(Continues)

TABLE 1 (Continued)

	Number/ sex/ ethnicity	Variant	Age of last examination	Hydrocephalus	Vision impairment	Hearing loss	Cardiovascular	Macrocephaly/ frontal bossing/ skeletal anomalies	Seizure/ Intellectual disability/MRI	Spasticity/ hypotonia	Detailed clinical information
Al-Dosari et al. (2013)[27]	22/Fetus/ Saudi	c.628C>T p.Gln210*	10 months	Yes	Yes	NA	Yes	NA/NA/NA	Yes/No/ Remarkable	No/Yes	Chorioretinal coloboma involving maculae bilaterally; small to moderate atrial septal defect with left to right shunt; MRI: extreme dilatation of the supratentorial ventricular system. The cerebral aqueduct was not significantly dilated. The corpus callosum could not be identified but the falx was present; Mother has a brother with CH, 24 y, with a ventriculoperitoneal shunt, at age 1 year, his IQ is estimated about 60. Her sister is now 12 years with CH who was operated on at the age of 1 month.
Al-Dosari et al. (2013)[27]	23/Fetus/ Saudi	c.628C>T p.Gln210*	NA	Yes	NA	NA	NA	NA/NA/NA	NA/NA/NA	NA/NA	Family has two abortions possibly affected by history

Abbreviations: ASD, atrial septal defect; CH, congenital hydrocephalus; CSF, cerebrospinal fluid; F, female; M, male; mat, maternal; NA, not information available; pat, paternal; VEP, visual evoked potential; VP, ventriculoperitoneal.

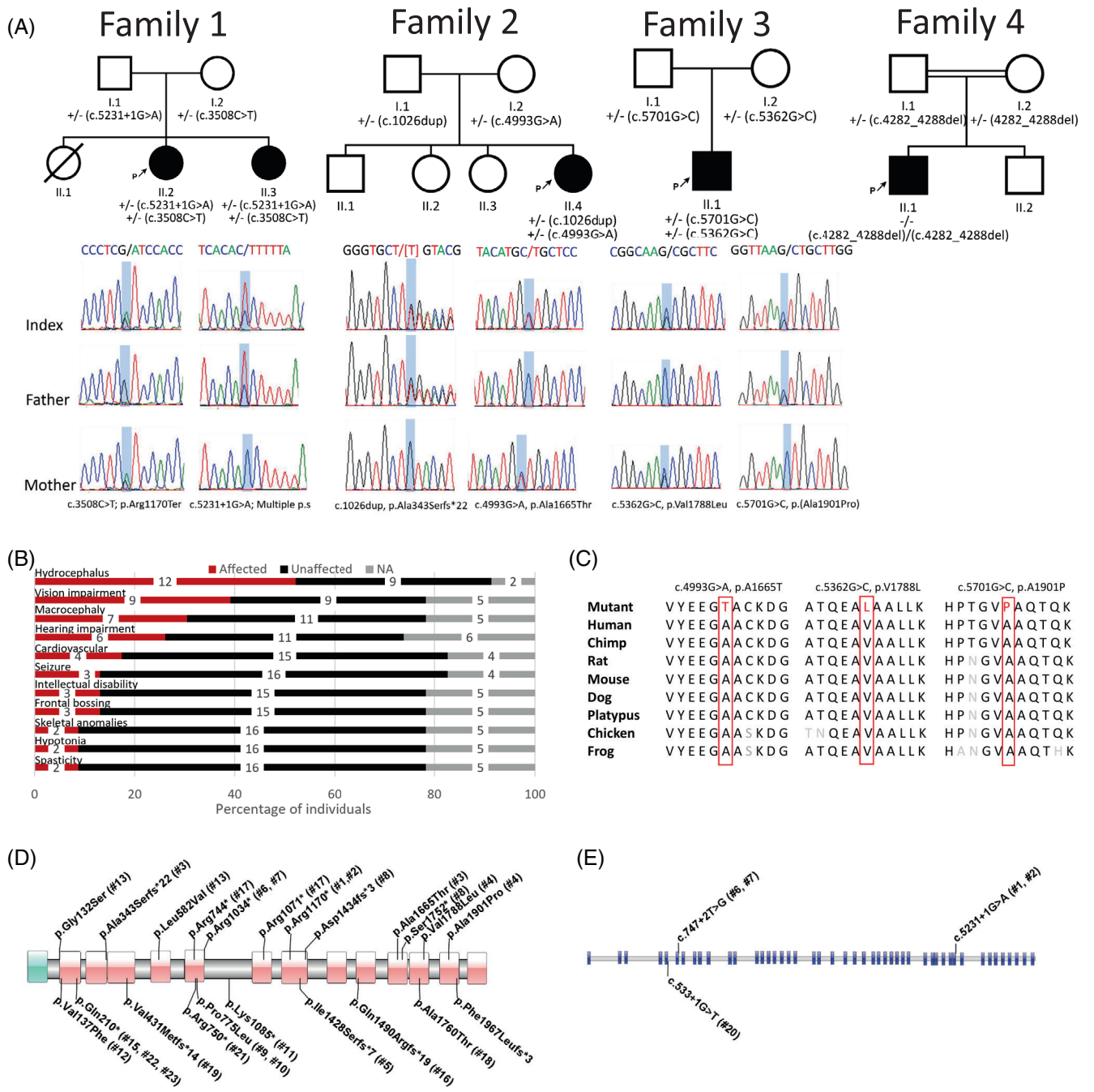

FIGURE 2 (A) Pedigrees and electropherograms of affected individuals. (B) Bar graph summarizing proportions of various clinical findings in patients with biallelic *MPDZ* variants. Red—affected, black—unaffected, gray—no information available. The *X* axis shows the percentage of patients and the number inside the bars shows the number of patients included in each of the categories. (C) Interspecies alignment was evaluated by Alamut Visual Plus v.1.6.1 and indicates the complete conservation down to invertebrates of the amino acid residues affected by the substitutions. (D) Overview of known and novel variants in *MPDZ* at the protein level (three variants are splicing which are shown in the cDNA schematic, see (E)). All variants were extracted from published papers or the current study. The pink region belongs to the PDZ domains (1–13) and the turquoise region is L27 domain. For each variant, the ID of patients are labeled after # and these IDs are based on Table 1. The variants in the upper part of the figure were detected in compound heterozygosity and those in the lower part of the figure were identified as homozygous variants. (E) Overview of known and novel variants in *MPDZ* that affect splicing. The blue regions represent exons. The variants in the upper part of the figure were detecting in compound heterozygosity while the variant at the lower part of the figure was homozygous. [Colour figure can be viewed at wileyonlinelibrary.com]

history is only remarkable for the proband's mother, apparently having a tendency towards walking on her toes (toe walking) since childhood but is otherwise unremarkable.

The proband was born at term by cesarean section (C-section) due to multiple previous maternal C-sections, without any complications and after an uneventful pregnancy. At birth, her weight was

3500 g and length was 52 cm. She was discharged from the maternity ward with her mother 72 h after birth. She subsequently presented normal psychomotor development, in both language and motor skills, having walked without support at 9 months of age. During her childhood and until the beginning of adolescence the only noticeable feature was toe-walking. At 12 years of age, gait abnormalities were initially noted by her mother, not being perceived by the proband herself, and appeared to remain stable until 25 years of age when her walking difficulty began to progress and lower limb spasticity was noticed. Her gait difficulties worsened progressively and by 32 years of age, she needed a walking aid in the form of crutches. She presently uses a wheelchair for long distances and two-point crutches for short distances. She also complains of urinary urgency and occasional urinary incontinence. She has no previous medical history of seizures, hospital admissions or surgeries. Her neurological examination disclosed bilateral lower limb spasticity, with hyperreflexia and positive bilateral Babinsky sign, characterizing a spastic paraparesis. She has no upper limb compromise and cognition is normal.

Previous examinations included normal fundoscopy and visual campimetry; a visual evoked potential test disclosing bilaterally increased P100 wave latency with normal amplitude; an ABR with widened I–V interpeak interval on the left and normal values on the right; an electromyography demonstrating mildly decreased right and left fibular nerves and left median nerve amplitudes; normal serological and biochemistry cerebrospinal fluid tests; a normal echocardiogram, as well as abdominal, kidney and urinary tract ultrasounds; and a cystography showing an overactive neurogenic bladder. Brain MRI with spectroscopy disclosed bilateral tenuous T2 and Flair white matter hyperintensities in the cerebral hemispheres and anterior portion of the corpus callosum, with reduced values of fractional anisotropy associated with increased myo-inositol levels in spectroscopy, suggestive of myelin sheath lesion, and mild "ex-vacum" lateral ventricle enlargement.

3.6 | Family 3

The proband in Family 3 is a male child evaluated at 3 years of age due to concerns of abnormal walking positions (Figure 2A). Neurological examination revealed the presence of spastic quadriplegia of cerebral palsy. CT and EEG performed during 3 years of age revealed no abnormalities. He is the only affected child in the family and was born full-term via vaginal delivery with no complications.

3.7 | Family 4

The proband in Family 4 is a 4-year-old boy with an unremarkable family history except parental consanguinity (Figure 2A). He was diagnosed with hydrocephalus prenatally. There was no history of maternal illness or substance use during pregnancy. He was born at 37 weeks and 4 days of gestation with a birth weight of 3695 g by C-section because of cephalo-pelvic discongruence. A postnatal MRI showed ventriculomegaly with absent septum pellucidum, broad interthalamic connection and hypoplastic optic nerve and chiasm and a diagnosis of septo-optic dysplasia was made. Epileptic seizures started at the age of 1 year. He was treated with lacosamide and lamotrigine. At the age of 4 years, bilateral macular coloboma were noted. He has a vision of 2/7.5 bilateral. He visited a medical day care because of developmental delay. Physical examination showed a height of 114.1 cm (+0.2 SD), weight of 21.0 kg (+0.7 SD) and head circumference of 54 cm (+1.9 SD). He has a triangular face with a high, broad, and prominent forehead and a pointed chin, hypertelorism with a broad nasal bridge and a narrow mouth. No other abnormalities were noted.

3.8 | Genetic analysis

The DNAs of probands from the four unrelated families (Family 1 II-2, Family 2 II-4, Family 3 II-1, Family 4 II-1) revealed variants in *MPDZ* (NM_001378778.1). The proband in Family 1 was identified with compound heterozygous variants including a maternally inherited c.3508C>T, p.Arg1170* nonsense variant in exon 25 with a minor allele frequency (MAF) of 0.00002567 in gnomAD (with 39 carriers) and a paternally inherited c.5231+1G>A, p.? canonical splice variant in intron 38, absent in gnomAD. The proband in Family 2 also presented compound heterozygous variants including a paternally inherited c.1026dupA, p.Ala343Serfs*22 frameshift variant in exon 8, absent in gnomAD, and a maternally inherited c.4993G>A, p.Ala1665Thr missense variant in exon 37 with a MAF of 0.00001611 in gnomAD (with 26 carriers). The proband in Family 3 was identified with compound heterozygous missense variants including a maternally inherited c.5362G>C, p.Val1788Leu variant in exon 39 with a MAF of 0.000001371 in gnomAD (with two carriers) and a paternally inherited c.5701G>C, p.Ala1901Pro variant in exon 43 with a MAF of 0.000001592 in gnomAD (with one carrier). The proband in Family 4 presented a homozygous frameshift variant c.4282_4288del, p.Ile1428Serfs*7 located in exon 30 that is absent in gnomAD. Previous genetic testing in this family was performed analyzing *HESX1* and *SOX2*, which revealed no abnormalities. Array analysis revealed a 12q12 deletion (chr12:40,562,013-40,774,520, GRCh37) that was inherited from the unaffected mother.

3.9 | Mini-gene assay

In vitro RNA studies of the c.5231+1G>A variant impacting a highly conserved donor splice site in intron 38 identified aberrant splicing in this region. The wild-type control showed evidence of alternative splicing (four different splice products) between exons 37 and 38. This result is consistent with the splicing model predicted by the Genotype-Tissue Expression (GTEx) portal (https://gtexportal.org/home/gene/MPDZ). Based on this portal, 13 different transcripts use these two exons, with one of these transcripts (ENST00000438511.5) skipping exon 37. Figure 3 shows four different splicing outcomes in this region, with all of them using the donor site in intron 38. Four

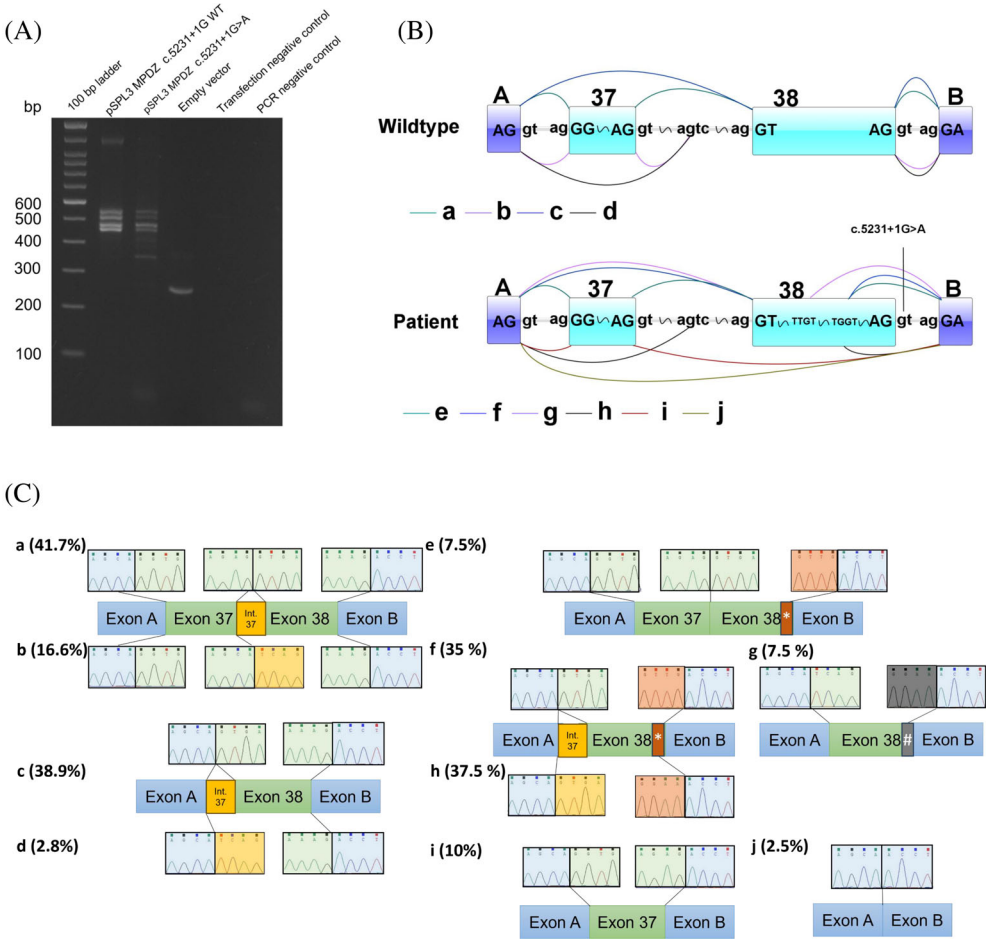

FIGURE 3 (A) Gel electrophoresis of the RT-PCR from the wild-type control, the c.5231+1G>A variant, and empty pSPL3 vector amplicons, as well as transfection negative and PCR negative controls. (B, C) The vector construct of the *in vitro* splice assay illustrates the wild-type or mutant amplicons inserted between exons A and B of the pSPL3 vector with a splicing schematic of the wild-type allele (upper B) and c.5231+1G>A variant (lower B). The wild-type construct shows four alternative splicing isoforms (a–d). The c.5231+1G>A variant activates two cryptic donor splice sites in exon 38 (e, f, g, and h). The variant showed evidence of skipping exon 38 following the variant (i) and skipping of both exons 37 and 38 (j). The empty vector control, with result summarized as equivalent to (j) and skipping of exons 37 and 38, performed as expected. The "*" in e and f indicates TGGT cryptic splice site and "#" in g shows the TTGT cryptic splice site in exon 38. The int. 37 refers to intron 37. [Colour figure can be viewed at wileyonlinelibrary.com]

alternative splicing amplicons were identified including amplicons showing evidence of: inclusion of both exons 37 and 38 (a), inclusion of both exons 37 and 38 but with a cryptic acceptor site activation in intron 37 (b), skipping of exon 37 (c), as well as skipping of exon 37 and usage of a cryptic acceptor site in intron 37 (d) (Figure 3B,C). However, the c.5231+1G>A variant indicates that the donor splice site in intron 38 is skipped and instead, either usage of two cryptic splice sites (e–h) or skipping of exon 38 occurred (i and j). The first cryptic splice site (TGGT) in exon 38 causes a frameshift variant: g.13121740_13121746del, r.5227_5231+2del, p.Asn1745Tyrfs*36. The second cryptic splice site in this exon, TTGT, causes an inframe deletion: g.13121739_13121749del, c.5223_5231+2del, p.Gly1742_Arg1744del. The skipping of exon 38 causes another frameshift variant: g.13121741_13121934del, c.5041_5231+3del, p.Asn1681Lysfs*38. TA cloning of the amplicon pool approximated the proportion of alternatively spliced amplicons in this region. The percentage of four different splicing outcomes from 36 clones for the wild-type are 41.7%, 16.6%, 38.9% and 2.8% for a-d, respectively (Figure 3C). The percentage of the six different amplicons from 43 clones for the c.5231+1G>A variant are: 7.5%, 35%, 7.5%, 37.5%, 10%, and 2.5%, for e, f, g, h, i, and j, respectively.

3.10 | ABR analysis in a murine model

As part of the International Mouse Phenotyping Consortium (IMPC) programme (https://www.mousephenotype.org/), a *Mpdz* knockout mouse model (*Mpdz*$^{em1(IMPC)J}$) was generated at the Jackson Laboratory employing CRISPR/Cas9-mediated genome editing.[28,29] This resulted in a non-homologous end joining event involving exon 6 of the *Mpdz* gene, leading to a 136 bp deletion coupled with a 29 bp insertion, which is predicted to cause a frameshift and early truncation (Figure 4A). Mice homozygous for this allele are viable and so were

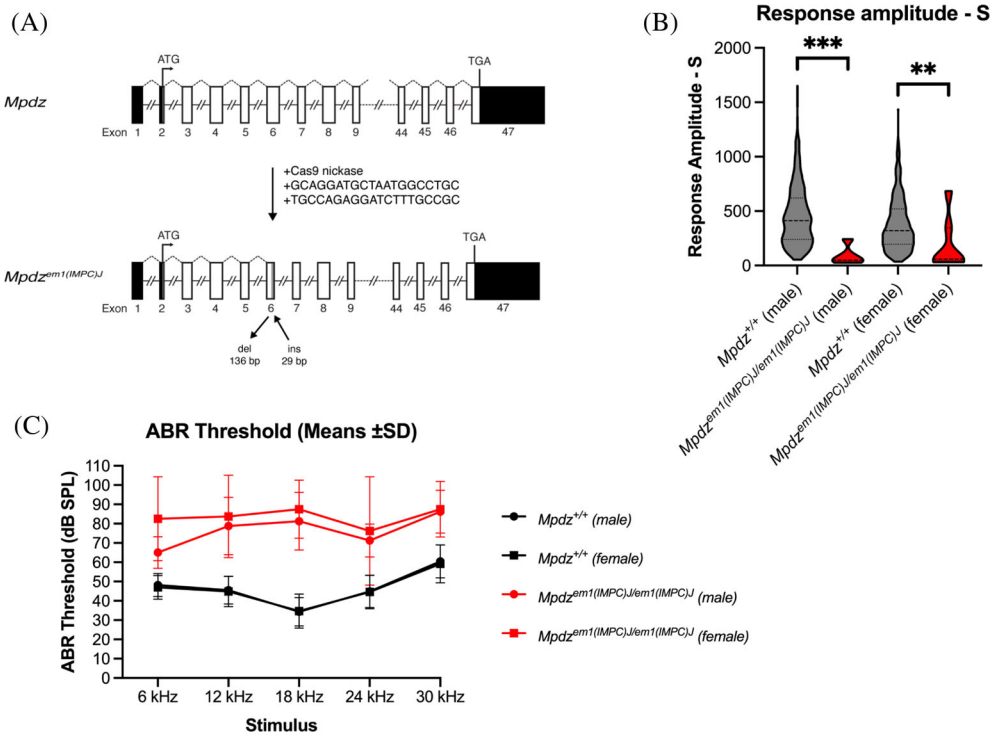

FIGURE 4 *Mpdz* knockout mice exhibit phenotypes consistent with hearing loss. (A) Schematic of the *Mpdz*$^{em1(IMPC)J}$ allele. (B) Chart showing the IMPC-derived data from an acoustic startle phenotyping assay measuring the Response amplitude—S in 7 female and 5 male *Mpdz* mutant mice compared to 489 female and 476 male wild-type controls. (C) Chart showing the IMPC-derived ABR threshold data in response to frequency specific acoustic stimuli in 4 female and 4 male *Mpdz* mutant mice compared to 606 female and 591 male wild-type controls. $^{**}p < 0.01$; $^{***}p < 0.001$. [Colour figure can be viewed at wileyonlinelibrary.com]

subject to the IMPC adult mouse phenotyping pipeline that includes an acoustic startle (Response amplitude—S) test at 10-weeks of age and an auditory brainstem response (ABR) test at 14-weeks of age. As part of the programme, phenotyping data generated from knockout mice can be compared with a running wild-type baseline of "normal" values for each test. At 10-weeks of age, in response to a 110 dB sound stimulus both male and female homozygous *Mpdz* knockout mice exhibit a significantly reduced startle reflex compared to wild-type mice (Figure 4B). At 14-weeks of age, both male and female homozygous *Mpdz* knockout mice exhibit elevated ABR hearing thresholds at all frequencies tested compared to wild-type mice (Figure 4C). Together these data indicate that *Mpdz* is critical for hearing in mice, and indicate that this model could be a valuable tool to investigate the pleiotropic and mechanistic effects of this gene.

4 | DISCUSSION

Biallelic variants in *MPDZ* have been implicated in a spectrum of phenotypes, but few functional studies have been performed to elucidate the disease mechanisms particularly for hydrocephalus and hearing impairment.[6–8] Here, we studied four unrelated families exhibiting a spectrum of phenotypes and identified novel variants in *MPDZ*. Initially, *MPDZ* was primarily associated with congenital hydrocephalus, encompassing a broad range of severities from stillbirth to severe congenital hydrocephalus.[27] However, subsequent identification of disease-causing variants in *MPDZ* revealed additional features, including vision impairment, hearing impairment, cardiac abnormalities, controllable seizure, mild intellectual disability,[24] lung hypoplasia, malrotation of the gut, and multicystic dysplastic kidney (Figure 2B).

Eleven out of 25 variants aggregated from the literature and current study were previously deposited in ClinVar (Figure 2D,E). In total, ClinVar submissions currently report 84 pathogenic/likely pathogenic *MPDZ* variants, including 35 frameshift, 28 nonsense, and 21 splicing variants, albeit with zygosity not provided (accessed February 2024). Remarkably, only 20 variants are explicitly associated with non-syndromic hydrocephalus, while the remainder are described as not provided/Inborn genetic diseases. Furthermore, there are 799 missense variants that are all classified as variants of uncertain significance (VUS). While this "VUS-explosion" is not exclusively unique to *MPDZ*, this suggests that the existing gaps of knowledge from both the mechanistic and clinical sides are in dire need of expansion in order to identify potential patients from this VUS-pool. Additionally, the under-characterized gene-phenotype description in key databases such as OMIM may further serve as a hurdle to the full appreciation of *MPDZ*-spectrum phenotypes. In our systematic review of the literature, we aimed to increase awareness of the current state of knowledge pertaining to a vast array of possible phenotypes.

Understanding the mechanisms of tissue specificity in heritable diseases remains a significant challenge. For instance, *RB1* is a well-known cell cycle gene but perturbations only cause retinoblastoma despite its broader cellular functions.[30] Although initial reports have suggested that severe hydrocephalus was caused by nonsense variants in *MPDZ*,[27] our study and very recent publications reveal that a variety of variants distributed from exons 5 to 45 may cause a wide range of phenotypes including a milder presentation. In our study, a homozygous LOF variant was identified in a patient with a severe phenotype involving hydrocephalus, vision impairment, macrocephaly and seizures. Another family presented with affected individuals with two LOF variants (nonsense and splicing variants, located in exon

25 and intron 38, respectively) that were associated with mild hydrocephalus, hearing loss and cardiac issues. In contrast, other compound heterozygous variants (frameshift [exon 7] and missense variants [exon 12]) in Family 2 and two missense variants (exons 12 and 14) in Family 3 were associated with spasticity. We analyzed the variant region and observed an evolutionary conserved region (Figure 2C). In the literature, compound heterozygous variants (splicing [exon 5] and missense variants [exon 14]) demonstrated external hydrocephalus with mild dilatation of lateral and third ventricles without other abnormal features (including vision and hearing impairment).[23] Recently, Zhang et al. has demonstrated that two LOF variants (nonsense [exon 39] and frameshift [exon 31]) only caused bilateral macular coloboma.[19] Additionally, Iyengar et al.[18] reported two affected siblings with variable structural abnormalities of the retina caused by compound heterozygous variants (nonsense [exon 22] and splicing [intron 6]).[18] One study described 10 heterozygous variants associated with retinitis pigmentosa and Leber congenital amaurosis, but this study had a methodological limitation, and it was not fully supporting the diagnosis.[31]

Based on the literature, two missense variants with a mild phenotype have been described: a homozygous missense variant p.Pro775Leu causing only hearing loss in a Pakistani family,[20] as well as a different missense variant p.Val137Phe causing hearing loss and congenital hereditary endothelial dystrophy in an Iranian family.[22] Additionally, Al-Jezawi et al.[23] identified two compound heterozygous novel variants (c.394G>A and c.1744C>G) in a patient with macrocephaly and communicating hydrocephalus. The in vitro functional study of the c.394G>A genetic variant revealed exon 5 skipping. Notably, this variant has a ClinVar entry (variation ID: 992337) with conflicting classifications of pathogenicity, being reported both as a VUS and likely pathogenic. Interestingly, the general population (gnomAD V.4) shows an entry with a homozygous status for this variant. To address this discrepancy, it is possible that this variant may only cause disease when combined with another pathogenic variant. Therefore, we recommend further in vivo functional studies to elucidate the role of both variants detected in this study. In our current study, we have identified two missense variants *in trans* (c.5362G>C and c.5701G>C) in a patient (F3, II-1) primarily affected by spasticity. Utilizing in silico tools, we predict that both variants are damaging, and interestingly, they are ultra-rare in the general population (gnomAD v.4). As, we detected another patient (F2, II-4) with spasticity caused by a compound heterozygous combination of variants (a frameshift and a missense), based on this finding, we hypothesize that the compound heterozygosity involving two missense variants may lead to a similar phenotype in patient F3, II-1. However, since this is the initial description of this phenotype for this specific gene, we recommend further functional studies to confirm the pathogenic impact of these missense variants in this patient. The variability in *MPDZ*-related phenotypes, ranging from mild to severe, may be attributed to several factors, including the presence of multiple transcripts (18 isoforms with 10 protein coding isoforms based on Ensembl) and/or regulation by NMD, which generally targets stop codons in both mutated and normal transcripts that adhere to the 50-nucleotide rule.[32] For instance, based on GTEx, six transcripts in *MPDZ* do not use a common last exon that is used in the MANE transcript. However, this hypothesis remains to be clarified via functional studies.

MPDZ functions as a scaffold protein for tight-junction-related proteins, adherens junction proteins, and transmembrane receptors. It comprises 13 PDZ domains that interact with the ion channel subunit C-terminal tail sequences and G-protein coupled receptors. Functional studies in *Mpdz*$^{-/-}$ mice implicate its role in ependymal and/or choroid plexus dysfunction, potentially explaining the brain abnormalities associated with *MPDZ* variants.[7] Furthermore, it has been demonstrated that *Mpdz* plays a role at the hair cell apical membrane where it colocalizes with MAGUK p55 subfamily member 5 (MPP5) and Crumbs protein CRB3, offering insight into its potential function in the inner ear.[8] Family 1 in this study supports the role of *MPDZ* in hearing. Nevertheless, the function of missense/inframe variants and the role of specific domains remains poorly understood.

In conclusion, our review summarized the various genotypes and phenotypes related to *MPDZ*. This review also reports novel variants in *MPDZ* with detailed phenotypic information. To the best of our knowledge, we highlight that biallelic variants in *MPDZ* can primarily cause spasticity in 8% of patients. Current evidence suggests that the spectrum of phenotypes may be influenced by location within the gene. Continued evaluation of new cases and functional studies on missense variants are essential for elucidating the precise roles of different domains and variant type on *MPDZ*-related phenotypes.

AUTHOR CONTRIBUTIONS

BV and AR conceptualized the study and designed the experiments. OB collected clinical information and conducted WES and segregation studies in Family 1. FPM and FK collected clinical information and conducted WES and segregation studies in Family 2. SB, CZ, YX, and MCK collected clinical information, and conducted WES and segregation studies in Family 3. AVS collected clinical information and conducted WGS in Family 4. MRB performed the analysis of data from the knockout murine model. BV and AR performed the systematic literature review. BV and AR prepared the complete first draft of the manuscript. The manuscript was reviewed and approved by all authors.

ACKNOWLEDGEMENTS

The authors thank the families for their participation in this study. This study was supported by Intramural Funding (fortüne) at the University of Tübingen (2545-1-0), the Ministry of Science, Research and Art Baden-Württemberg and the German Research Foundation DFG VO 2138/7-1 grant 469177153 (BV) and the National Nature Science Foundation of China (U21A20347). BV is a member of the European Reference Network on Rare Congenital Malformations and Rare Intellectual Disability (ERN-ITHACA) (EU Framework Partnership Agreement ID: 3HP-HP-FPA ERN-01-2016/739516). We acknowledge support by the Open Access Publication Funds of the University of Göttingen. Open Access funding enabled and organized by Projekt DEAL.

CONFLICT OF INTEREST STATEMENT

The authors declare no conflict of interest.

DATA AVAILABILITY STATEMENT

The data that support the findings of this study are openly available in Leiden Open Variation Database (LOVD), variant IDs #0000960145-#0000960151.

ORCID

Changlian Zhu https://orcid.org/0000-0002-5029-6730
Barbara Vona https://orcid.org/0000-0002-6719-3447

REFERENCES

1. Ullmer C, Schmuck K, Figge A, Lübbert H. Cloning and characterization of MUPP1, a novel PDZ domain protein. *FEBS Lett*. 1998;424(1–2):63-68.
2. Simpson EH, Suffolk R, Jackson IJ. Identification, sequence, and mapping of the mouse multiple PDZ domain protein gene, Mpdz. *Genomics*. 1999;59(1):102-104.
3. Guillaume JL, Daulat AM, Maurice P, et al. The PDZ protein mupp1 promotes Gi coupling and signaling of the Mt1 melatonin receptor. *J Biol Chem*. 2008;283(24):16762-16771.
4. Krapivinsky G, Medina I, Krapivinsky L, Gapon S, Clapham DE. SynGAP-MUPP1-CaMKII synaptic complexes regulate p38 MAP kinase activity and NMDA receptor-dependent synaptic AMPA receptor potentiation. *Neuron*. 2004;43(4):563-574.
5. Tetzlaff F, Adam MG, Feldner A, et al. MPDZ promotes DLL4-induced notch signaling during angiogenesis. *Elife*. 2018;7:7.
6. Feldner A, Adam MG, Tetzlaff F, et al. Loss of Mpdz impairs ependymal cell integrity leading to perinatal-onset hydrocephalus in mice. *EMBO Mol Med*. 2017;9(7):890-905.
7. Yang J, Simonneau C, Kilker R, et al. Murine MPDZ-linked hydrocephalus is caused by hyperpermeability of the choroid plexus. *EMBO Mol Med*. 2019;11(1):1-19.
8. Jarysta A, Tarchini B. Multiple PDZ domain protein maintains patterning of the apical cytoskeleton in sensory hair cells. *Development*. 2021;148(14):1-14.
9. Sobreira N, Schiettecatte F, Valle D, Hamosh A. GeneMatcher: a matching tool for connecting investigators with an interest in the same gene. *Hum Mutat*. 2015;36(10):928-930.
10. McKenna A, Hanna M, Banks E, et al. The genome analysis toolkit: a MapReduce framework for analyzing next-generation DNA sequencing data. *Genome Res*. 2010;20(9):1297-1303.
11. Li H, Durbin R. Fast and accurate long-read alignment with Burrows-Wheeler transform. *Bioinformatics*. 2010;26(5):589-595.
12. Rad A, Altunoglu U, Miller R, et al. MAB21L1 loss of function causes a syndromic neurodevelopmental disorder with distinctive cerebellar, ocular, craniofacial and genital features (COFG syndrome). *J Med Genet*. 2019;56(5):332-339.
13. Karczewski KJ, Francioli LC, Tiao G, et al. The mutational constraint spectrum quantified from variation in 141,456 humans. *Nature*. 2020;581(7809):434-443.
14. Ioannidis NM, Rothstein JH, Pejaver V, et al. REVEL: an ensemble method for predicting the pathogenicity of rare missense variants. *Am J Hum Genet*. 2016;99(4):877-885.
15. Schubach M, Maass T, Nazaretyan L, Röner S, Kircher M. CADD v1.7: using protein language models, regulatory CNNs and other nucleotide-level scores to improve genome-wide variant predictions. *Nucleic Acids Res*. 2024;52(D1):D1143-D1154.
16. Rad A, Schade-Mann T, Gamerdinger P, et al. Aberrant COL11A1 splicing causes prelingual autosomal dominant nonsyndromic hearing loss in the DFNA37 locus. *Hum Mutat*. 2021;42(1):25-30.
17. Tompson SW, Young TL. Assaying the effects of splice site variants by exon trapping in a mammalian cell line. *Bio Protoc*. 2017;7(10):1-18.
18. Iyengar R, Deardorff M, Schmidt R, Nagiel A. Retinal manifestations in autosomal recessive MPDZ maculopathy: report of two cases and literature review. *Ophthalmic Genet*. 2023;44(6):572-576.
19. Zhang S, Zhang F, Wang J, et al. Novel compound heterozygous variations in MPDZ gene caused isolated bilateral macular Coloboma in a Chinese family. *Cells*. 2022;11(22):3602.
20. Bharadwaj T, Schrauwen I, Rehman S, et al. ADAMTS1, MPDZ, MVD, and SEZ6: candidate genes for autosomal recessive nonsyndromic hearing impairment. *Eur J Hum Genet*. 2022;30(1):22-33.
21. Bertoli-Avella A M, Beetz C, Ameziane N, et al. Successful application of genome sequencing in a diagnostic setting: 1007 index cases from a clinically heterogeneous cohort. *Eur J HumGenet*. 2020;29(1):141-153.
22. Moazzeni H, Javadi MA, Asgari D, et al. Observation of nine previously reported and 10 non-reported SLC4A11 mutations among 20 Iranian CHED probands and identification of an MPDZ mutation as possible cause of CHED and FECD in one family. *Br J Ophthalmol*. 2020;104(11):1621-1628.
23. Al-Jezawi NK, Al-Shamsi AM, Suleiman J, et al. Compound heterozygous variants in the multiple PDZ domain protein (MPDZ) cause a case of mild non-progressive communicating hydrocephalus. *BMC Med Genet*. 2018;19(1):34.
24. Harripaul R, Vasli N, Mikhailov A, et al. Mapping autosomal recessive intellectual disability: combined microarray and exome sequencing identifies 26 novel candidate genes in 192 consanguineous families. *Mol Psychiatry*. 2018;23(4):973-984.
25. Shaheen R, Sebai MA, Patel N, et al. The genetic landscape of familial congenital hydrocephalus. *Ann Neurol*. 2017;81(6):890-897.
26. Saugier-Veber P, Marguet F, Lecoquierre F, et al. Hydrocephalus due to multiple ependymal malformations is caused by mutations in the MPDZ gene. *Acta Neuropathol Commun*. 2017;5(1):36.
27. Al-Dosari MS, Al-Owain M, Tulbah M, et al. Mutation in MPDZ causes severe congenital hydrocephalus. *J Med Genet*. 2013;50(1):54-58.
28. Groza T, Gomez FL, Mashhadi HH, et al. The International Mouse Phenotyping Consortium: comprehensive knockout phenotyping underpinning the study of human disease. *Nucleic Acids Res*. 2023;51(D1):D1038-D1045.
29. Bowl MR, Simon MM, Ingham NJ, et al. A large scale hearing loss screen reveals an extensive unexplored genetic landscape for auditory dysfunction. *Nat Commun*. 2017;8(1):886.
30. Hekselman I, Yeger-Lotem E. Mechanisms of tissue and cell-type specificity in heritable traits and diseases. *Nat Rev Genet*. 2020;21(3):137-150.
31. Ali M, Hocking PM, McKibbin M, et al. Mpdz null allele in an avian model of retinal degeneration and mutations in human leber congenital amaurosis and retinitis pigmentosa. *Invest Ophthalmol Vis Sci*. 2011;52(10):7432-7440.
32. Maquat LE. Nonsense-mediated mRNA decay: splicing, translation and mRNP dynamics. *Nat Rev Mol Cell Biol*. 2004;5(2):89-99.

SUPPORTING INFORMATION

Additional supporting information can be found online in the Supporting Information section at the end of this article.

How to cite this article: Rad A, Bartsch O, Bakhtiari S, et al. Expanding the spectrum of phenotypes for *MPDZ*: Report of four unrelated families and review of the literature. *Clinical Genetics*. 2024;1-14. doi:10.1111/cge.14563